Kinetics, Energetics, and Electronic Coupling of the Primary Electron Transfer Reactions in Mutated Reaction Centers of *Blastochloris viridis*

P. Huppman,* T. Arlt,* H. Penzkofer,* S. Schmidt,* M. Bibikova,† B. Dohse,† D. Oesterhelt,† J. Wachtveit,* and W. Zinth*

*Institut für BioMolekulare Optik, Sektion Physik, Ludwig-Maximilians-Universität, D-80538 München, Germany; and †Max-Planck-Institut für Biochemie, Am Klopferspitz 18a, D-82152 Martinsried, Germany

ABSTRACT Femtosecond spectroscopy in combination with site-directed mutagenesis has been used to study the dynamics of primary electron transfer in native and 12 mutated reaction centers of *Blastochloris* (*B*) (formerly called *Rhodopseudomonas*) *viridis*. The decay times of the first excited state P* vary at room temperature between of 0.6 and 50 ps, and at low temperatures between 0.25 and 90 ps. These changes in time constants are discussed within the scope of nonadiabatic electron transfer theory using different models: 1) If the mutation is assumed to predominantly influence the energetics of the primary electron transfer intermediates, the analysis of the room temperature data for the first electron transfer step to the intermediate $P^+B_A^-$ yields a reorganization energy $\lambda = 600 \pm 200\ cm^{-1}$ and a free energy gap ΔG ranging from $-600\ cm^{-1}$ to $800\ cm^{-1}$. However, this analysis fails to describe the temperature dependence of the reaction rates. 2) A more realistic description of the temperature dependence of the primary electron transfer requires different values for the energetics and specific variations of the electronic coupling upon mutation. Apparently the mutations also lead to pronounced changes in the electronic coupling, which may even dominate the change in the reaction rate. One main message of the paper is that a simple relationship between mutation and a change in one reaction parameter cannot be given and that at the very least the electronic coupling is changed upon mutation.

INTRODUCTION

The primary photochemical event during photosynthesis in bacteriochlorophyll-containing organisms is a light-induced charge separation within a transmembrane protein complex called the reaction center (RC). In purple bacteria the protein complex contains at least three protein subunits referred to as L, M, and H, according to their respective degrees of mobility in sodium dodecyl sulfate-polyacrylamide gels. Associated with the L and M subunits are the cofactors, consisting of four bacteriochlorophylls (BChl), two bacteriopheophytins (BPhe), one atom of nonheme ferrous iron, and two quinones. Most investigations dealing with purple bacterial photosynthesis were performed on the RC of *Rhodobacter* (*Rb.*) *sphaeroides, Rb. capsulatus*, and *Blastochloris* (*B*., formerly called *Rhodopseudomonas*) *viridis*, respectively. (While *Rb. sphaeroides* and *Rb. capsulatus* contain BChl-*a* and BPhe-*a* as tetrapyrroles in *B. viridis* BChl-*b* and BPhe-*b* are incorporated.) The cofactors are arranged in two branches with an approximate C_2-symmetry called the A and B branch (for details of the crystal structure see Ermler et al. (1994) and Fig. 1).

The dynamics of the light-induced electron transfer steps have been investigated by time-resolved spectroscopy over the last two decades. Optical excitation leads to the transfer of an electron away from a pair of strongly coupled bacteriochlorophyll molecules, the so-called special pair P in ~2.2 ps (Breton et al., 1986; Dressler et al., 1991). Improved techniques yielded further details about the decay of the first excited electronic state P*: Deviations from a

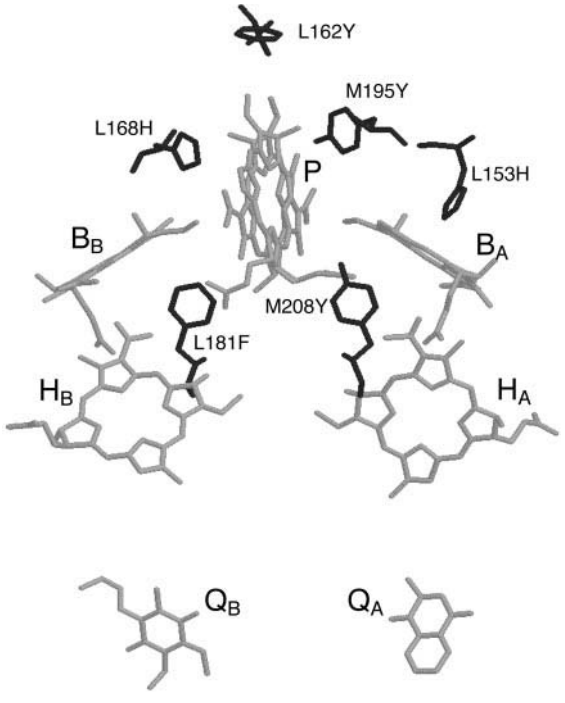

FIGURE 1 Schematic view of the co-factors and the mutated amino acids in the RC form *B. viridis*.

Submitted August 7, 2001 and accepted for publication February 19, 2002.

J. Wachtveitl's present address is Institut für Physikalische und Theoretische Chemie, Johann-Wolfgang-Goethe-Universität, Marie-Curie-Str. 11, D-60439 Frankfurt, Germany.

Address reprint requests to W. Zinth, Institute für BioMolekulare Optik, Sektion Physik, Ludwig-Maximilians-Universität, Oettingenstr. 67, D-80538 München, Germany. Tel.: 0049-89-2180-9202; Fax: 0049-89-2180-9202; E-mail: zinth@physik.uni-muenchen.de.

0006-3495/02/06/3186/12 $2.00

monoexponential decay (Du et al., 1992; Hamm et al., 1993; Jia et al., 1993; Ogrodnik et al., 1994; Beekman et al., 1995) and oscillatory contributions at low temperatures (Vos et al., 1991, 1992, 1993; Spörlein et al., 1998) were also reported. The arrival of the electron at the bacteriopheophytin H_A on the A branch is observed in the time range of 3 to 4 ps after electronic excitation (Breton et al., 1986; Fleming et al., 1988; Holzapfel et al., 1989, 1990). In a series of publications it has been established that the reaction does not directly lead to $P^+H_A^-$ and that the bacteriochlorophyll B_A acts as an intermediary electron carrier (Holzapfel et al., 1989, 1990; Dressler et al., 1991; Schmidt et al., 1993; Arlt et al., 1993).

For the RCs of *Rb. sphaeroides* and *Rb. capsulatus*, investigations of mutant or chromophore exchanged RCs yielded information on the energetics and the mechanism of photosynthetic electron transport (Bylina et al., 1988; Nagarajan et al., 1990, 1993; Gray et al., 1990; Finkele et al., 1990; Lauterwasser et al., 1991; Farchaus et al., 1993; Jia et al., 1993; Heller et al., 1995; Woodbury et al., 1995; Huber et al., 1998; Spörlein et al., 2000). For example, RCs with exchanged pheophytins allow to estimate the free energy difference between P* and $P^+B_A^-$; a value of approximately $-450\ cm^{-1}$ was found in *Rb. sphaeroides* (Schmidt et al., 1993, 1994).

For *B. viridis* it has been shown that electron transfer times are in the same range as those observed in *Rb. sphaeroides* (Dressler et al., 1991). In RCs of *B. viridis* the first electron transfer step is similar, the second one slightly accelerated (0.65 ps instead of 0.9 ps) (Arlt et al., 1993). Considering the differences between *B. viridis* and *Rb. sphaeroides* RC in pigment (BChl-*b* versus BChl-*a*) and protein composition (only 50–60% sequence identity of the L- and M-subunits), the good agreement in the time constants is surprising.

While mutant RCs of *Rb. sphaeroides* and *Rb. capsulatus* have now been available for over a decade, the construction of a variety of mutant RCs of *B. viridis* has been achieved only in the midnineties (Laußermair and Oesterhelt, 1992; Dohse et al., 1995).

To study the energetics and transfer mechanism in RC of *B. viridis* in more detail, we used femtosecond spectroscopy at different temperatures together with site-directed mutagenesis. Most calculations dealing with the primary photosynthetic reaction are carried out on the basis of an improved structure of *B. viridis* (resolution of 2.3 Å (Lancaster and Michel, 1997)), and in some cases the structure of the mutant RC from *B. viridis* is now available (Kuglstatter et al., 1999; Lancaster et al., 2000). Therefore, our experimental results can be directly compared with theoretical calculations (Parson and Warshel, 1993).

MATERIALS AND METHODS

Native and mutant RCs of *B. viridis* were prepared as described previously (Ditta et al., 1985; Dressler et al., 1991; Laußermair and Oesterhelt, 1992). Electrochemical redox titrations were carried out with the set-up described in Wachtveitl et al. (1993b).

The transient absorption experiments in the subpicosecond time range were performed at room temperature by a laser-amplifier system based on a CPM dye laser (Schmidt et al., 1993). The basic features of the system are: a repetition rate of 50 Hz, an excitation wavelength $\lambda_{exc} = 960$ nm in the low energy $Q_Y(P)$ band, probing pulses in the range between 660 and 1050 nm, and a width of the instrumental response function of 250 fs.

The experiments were performed with parallel polarization between pump and probe pulses. For the room temperature experiments, the sample was held in an optical cell with a 1-mm pathlength and stirred continuously. For measurements at cryogenic temperatures, the samples contained 52% (v/v) glycerol as a cryoprotector and 0.32 M benzyl viologen to prereduce the quinones thus avoiding the accumulation of long-lived photoproducts. The addition of glycerol and benzyl viologen slowed down the electron transfer dynamics by ~10% compared with measurements without glycerol and benzyl viologen. The concentration of the RCs was adjusted to yield a sample transmission of $T \approx 10\%$ at 960 nm ($\approx 50\ \mu M$). Approximately 15% of the RCs in the irradiated volume were excited. For modeling of the ultrafast reaction dynamics, nonadiabatic electron transfer (ET) theory (Marcus and Sutin, 1985; Bixon et al., 1991, 1995) is applied and the reactions are described by a rate equation system (Schmidt et al., 1995). The intermediates I_i and I_j of the ET processes are connected by microscopic rates γ_{ij}. The rates measured in the time-resolved experiments correspond to the eigenvalues $k_i = 1/\tau_i$ of the rate matrix. They are not identical with the microscopic rates when branching, backward rates, or recombination processes are involved (Schmidt et al., 1995). For the theoretical modeling of the transient absorption data a sum of exponentials weighted with amplitudes and convoluted with the instrumental response function is used.

RESULTS

Investigated mutants

In this study we concentrated on RCs mutated around the special pair and the adjacent monomeric BChl-*b* pigments B_A and B_B. The positions of the exchanged amino acids within the RC are depicted in Fig. 1. The mutants can be divided into four groups.

RCs with a modified hydrogen bonding pattern to the special pair

There are three amino acids donating hydrogen bonds to the bacteriochlorophylls P_M (= P_A) and P_L (= P_B) of the special pair in *B. viridis* (Lancaster and Michel, 1997): tyrosine (Y) at position M195, threonine (T) at position L248, and histidine (H) at position L168. Raman spectroscopy on the corresponding mutants of *Rb. sphaeroides* showed that the exchange of histidine L168 with a nonpolar phenylalanine (F) removes a hydrogen bond and results in a dramatic decrease of the P/P^+ redox potential (Mattioli et al., 1995). In the case of *B. viridis* we investigated the mutants L168H → F (L168HF), M195Y → F (M195YF), M195Y → H (M195YH), and the double mutant L168HF/M195YF.

RCs mutated at the positions L181 and M208, key positions located between P, B_A and H_A, and P, B_B and H_B, respectively

In wild type (WT), we find a nonpolar phenylalanine at the inactive branch (position L181) and a polar tyrosine at the

active branch (position M208). Calculations from Parson and coworkers showed that the main effect of the polar tyrosine is to lower the energy level of $P^+B_A^-$ (Parson et al., 1990; Nagarajan et al., 1993). Thus, an exchange of a tyrosine for a nonpolar phenylalanine or leucine (L) should raise the energy level of $P^+B_A^-$. The investigated mutants are M208YF, M208YL, L181FY, and the double mutant L181FY/M208YF.

RC with a modified binding pocket of the bacteriochlorophyll B_A

Histidine L153 is known as the ligand of the Mg-atom of the bacteriochlorophyll B_A. The replacement of histidine by leucine leads to the incorporation of a bacteriopheophytin in the B_A-binding pocket of the L153HL mutant. The L153 mutants were discussed in detail elsewhere (Arlt et al., 1996b) and are presented here to complement the data set. We studied the mutants L153HL and L153HC.

RC mutated at position L162 located between the special pair P and the proximal heme c-559, which reduces the photooxidized special pair after primary charge separation

Mutations at this position are expected to have smaller, probably electrostatic effects on the energetics and the electron transfer rate from P to B/H. We investigated the mutants L162YF and L162YG.

Steady-state characterization

Optical absorption spectra

In general, the absorption spectra of mutant and WT RC are quite similar and spectral shifts occur only in the range of few nanometers, indicating that the structure of the protein near the chromophores is not drastically changed. Larger shifts are observed only in the $Q_Y(P)$ bands of the RCs with hydrogen bonds removed (group 1 mutants) and for the mutant L153HL, where the introduced bacteriopheophytin leads to a shift of the $Q_Y(B)$ band (~15 nm) towards shorter wavelengths (for details see Arlt et al. (1996b)). The peaks of the $Q_Y(P)$ absorption bands of the several mutants and the FWHM of these bands are given in Table 1. In the L168HF and M195YF mutants the $Q_Y(P)$ band is shifted by 30 to 35 nm, in the double mutant L168HF/M195YF a shift of ~65 nm is observed, i.e., the removal of one hydrogen bond from the special pair results in a shift of the $Q_Y(P)$ band of ~30 nm. In the RC of *Rb. sphaeroides* the corresponding value was roughly 20 nm (Mattioli et al., 1995). These changes in the optical spectra probably reflect an alteration of the electronic structure and/or different excitonic interaction within the special pair induced by the altered H bond pattern.

TABLE 1 Spectroscopic and redox properties of modified reaction centers

RC *B. viridis*	$\lambda_{max}(Q_Y(P))$ (nm)	$\Delta\lambda_{1/2}(Q_Y(P))$ (nm)	$\Delta U_{P/P+}$ [mV]	$\Delta\Delta G$ [cm^{-1}]
WT	968	84	0	0
L168HF	930	90	−80	−670
M195YF	949	81	−45	−370
L168HF/M195YF	900	120	−80	*
M195YH	940	86	+20	+170
L181FY	960	83	−25	−210
M208YF	969	82	+15	*
M208YL	966	89	+15	*
L181FY/M208YF	963	83	−25	*
L153HC	963	83	+2	+16
L153HL	963	85	0	−1600
L162YF	962	94	≈−5	−40
L162YG	960	83	+10	+80

Position (λ_{max}) and width (full width at half maximum, $\Delta\lambda_{1/2}$) of the Q_Y-absorption band. The P/P^+-redox midpoint potential ($\Delta U_{P/P+}$) is expressed as difference from the WT value of +520 mV. This value together with the contribution arising from chromophore modification (e.g., in L153HL RC) determines the change in free energy difference for the first electron transfer step according to Eqs. 7 and 8.

*$\Delta\Delta G$ cannot be calculated from Eq. 7 because additional changes are expected.

Electrochemical redox titrations

The redox midpoint potentials of the primary donor (P/P^+-potentials) of the various samples are also summarized in Table 1. The absolute value of the redox potential for the WT RC is 520 ± 10 mV. Table 1 shows that larger changes ($\Delta U_{P/P+} > 30$ mV) of the P/P^+-midpoint potential occur only in the mutants with altered hydrogen bonds. The removal of a hydrogen bond results in a decrease of the $\Delta U_{P/P+}$ in the range of 40 to 80 mV. A hydrogen bond obviously stabilizes the neutral state of the special pair P. However, comparing the values obtained for L168HF and the double mutant L168HF/M195YF we find that the effects are not additive. This indicates that additional structural changes are induced by the double mutation.

The mutants of the other groups show relatively small (group 2) or negligible (groups 3 and 4) differences in the P/P^+ redox potential. This observation supports calculations (Parson et al., 1990), which indicate that these mutations mainly influence the energy level of B_A or B_B but not of P.

Femtosecond spectroscopy

Time resolved experiments have been performed at probing wavelengths characteristic of the different ET steps (Dressler et al., 1991). For the modeling of the transient absorption changes we used time constants τ_i, $i = 1, \ldots 4$ connected to the different reaction steps (τ_1, decay of P^* and ET from P^* to B_A; τ_2, ET from B_A to H_A; τ_3, ET from H_A to Q_A; and τ_4, (= ∞), long lasting absorption changes). The set of time constants for each mutant was determined

TABLE 2 Electron transfer dynamics for native and mutated *B. viridis* reaction centers at room temperature

RC *B. viridis*	τ_1 (ps)	τ_{1A}/τ_{1B} (ps) ± 25%	$R = \frac{a_{1A}}{a_{1B}}$ ±30%	τ_2 (ps)	τ_3 (ps)
WT	3.5 ± 0.4	1.8/7.4	1.4	0.65 ± 0.3	220 ± 30
L168HF	1.1 ± 0.2	0.8/3.8	4.8	0.65 ± 0.1	200 ± 30
M195YF	3.1 ± 0.3	1.5/5.4	0.8	0.65 ± 0.3	150 ± 30
L168HF/M195YF	0.8 ± 0.2	0.6/3.2	3.0	0.65 ± 0.1	150 ± 30
M195YH	5.7 ± 0.5	3.5/14.5	2	0.65 ± 0.5	220 ± 30
L181FY	1.7 ± 0.2	1.15/4.5	2.8	0.65 ± 0.2	210 ± 30
M208YF	20 ± 3	8/30	0.3	-	200 ± 30
M208YL	29 ± 5	11/50	0.5	-	200 ± 30
L181FY/M208YF	8.2 ± 1.5	4.5/16	2.3	-	180 ± 30
L153HC	3.8 ± 0.4	2.5/10	3	0.65 ± 0.3	160 ± 30
L153HE	12 ± 1	7/40	2	-	170 ± 30
L153HL	3.5 ± 0.4	3/43	4	1.5 ± 0.6	140 ± 30
L162YF	3.5 ± 0.4	2.7/16	>4	0.65 ± 0.3	200 ± 30
L162YG	5.4 ± 0.5	3.3/18	2.6	0.65 ± 0.4	200 ± 30

The given decay constants result from a monoexponential (τ_1) or a biexponential (τ_{1A}, τ_{1B}) fit of the first electron transfer step $P^* \rightarrow P^+B_A^-$, R indicates the ratio of the respective amplitudes. Monoexponential functions are used to fit the transients for the second (τ_2) and third (τ_3) electron transfer steps.

globally from the data recorded at the different probing wavelengths. They are summarized in Table 2.

At certain probing wavelengths single reaction steps dominate the observed absorption changes: The population of the excited electronic level *P** of the special pair can be investigated via its stimulated emission (gain) in the long wavelength region of the special pair Q_Y-band (1020–1050 nm). Fig. 2 presents some examples of the detected transient absorption changes of the mutant RC. In general, monoexponential fit functions (time constant τ_1) do not reproduce all the details of the absorption changes related to the *P** decay. Thus, a biexponential fit function was used (time constants τ_{1A}, τ_{1B}), as has been successfully applied in previous studies (Jia et al., 1993; Hamm et al., 1993). Except for the mutants M195YF, M208YF, and M208YL the amplitude a_{1A} of the faster decay component dominates. Both the relative amplitudes a_{1A} and a_{1B} (of the time constants τ_{1A} and τ_{1B}) and the relative values of the time constants themselves determine the deviation from a monoexponential decay. The *P** population $N_{P*}(t)$ is given by:

$$N_{P*}(t) = a_{1A} \times \exp(-t/\tau_{1A}) + a_{1B} \times \exp(-t/\tau_{1B}) \quad (1)$$

Here a_{1A} and a_{1B} are the amplitudes of the two *P** decay times τ_{1A} and τ_{1B} with the normalization $N_{P*}(0) = 1$ or $a_{1A} + a_{1b} = 1$. Often, the monoexponential decay constants τ_1 are sufficient for a qualitative estimate for the lifetime of the excited electronic level *P**. The data evaluation reveals the qualitative trend that larger deviations from a monoexponential function were observed in the mutants with a slower *P** decay. This agrees well with results obtained on mutated RCs of *Rb. capsulatus* (Jia et al., 1993). The deviations from a monoexponential fit function are small for mutants showing a very fast decay (L168HF, L181FY, L168HF/M195YF).

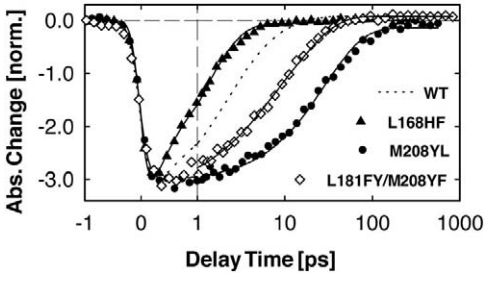

FIGURE 2 Transient absorption data (*circles, triangles, diamonds*) of different mutants and WT RC at 1050 nm (mutant L168HF, where the Q_y absorption peak is blueshifted at the corresponding wavelength 1020 nm). The solid curves are modeled using a biexponential decay. The modeled time constants τ_{1A} and τ_{1B} (see Eq. 1) and their amplitudes are given in Table 2. Note the linear scale for the delay times of <1 ps and the logarithmic scale at later delay times.

We find dominant decay times of *P** (see Table 2) between 0.6 and 50 ps (1.8 ps is the value for WT). The removal of a hydrogen bond to the special pair generally leads to an acceleration of the *P** decay (mutants L168HF, M195YF, and double mutant L168HF/M195YF). This double mutant shows the fastest *P** decay with $\tau_1 = 0.8$ ps (monoexponential fit) or $\tau_{1A} = 0.6$ ps (biexponential fit). Such a drastic acceleration by a factor 3 to 5 as compared with WT (monoexponential fit) was not observed for the corresponding mutants of *Rb. sphaeroides* (Woodbury et al., 1994; Murchison et al., 1993).

In qualitative agreement with the M208-mutants of *Rb. capsulatus* (Jia et al., 1993) and the M210-mutants of *Rb. sphaeroides* (Wachtveitl et al., 1998; Beekman et al., 1996; Finkele et al., 1990; Jia et al., 1993; Nagarajan et al., 1990) the replacement of the tyrosine (Y) at the position M 208 by a phenylalanine (F) or leucine (L) slows down the first electron transfer step by a factor of 6 to 10. In contrast, the

TABLE 3 Temperature dependence of primary electron transfer times

T [K]	*WT* (τ_{1A}, τ_{1B}) (ps)	a_{1A}/a_{1B}	L181FY (τ_{1A}, τ_{1B}) (ps)	a_{1A}/a_{1B}	L168HF (τ_{1A}, τ_{1B}) (ps)	a_{1A}/a_{1B}	M195YF (τ_{1A}, τ_{1B}) (ps)	a_{1A}/a_{1B}	M208YF (τ_{1A}, τ_{1B}) (ps)	a_{1A}/a_{1B}
30	1.1, 37	2.9	-	-	0.25, 1.7	1.9	-	-	9, 83	0.44
50	-	-	0.5, 1.3	2.5	-	-	1, 3.5	3.3	6, 74	0.4
70	1.2, 28	3.1	-	-	0.25, 1.5	2.0	-	-	-	-
80	-	-	-	-	-	-	-	-	11, 90	0.47
100	1.3, 24	3.5	0.6, 1.5	1.1	0.29, 2.4	3.9	1.1, 2.9	9.6	-	-
120	-	-	-	-	-	-	-	-	9, 90	0.44
130	-	-	-	-	0.32, 2.4	3.1	-	-	-	-
140	1.4, 21	2.8	-	-	-	-	-	-	-	-
150	-	-	0.8, 2.2	2.4	-	-	1.9, 6.3	1.6	-	-
155	-	-	-	-	0.36, 3.4	4.3	-	-	-	-
160	-	-	-	-	-	-	-	-	14,88	0.56
180	1.8, 19	2.7	-	-	0.35, 3.0	3.3	-	-	-	-
230	1.9, 17	2.1	1, 3.3	3.2	0.54, 1.6	2.3	-	-	11,61	0.25
270	2.1, 14	1.1	-	-	-	-	-	-	14, 47	0.49
295	2.2, 12	1.9	1.3, 4.2	1.6	0.72, 3.5	3.1	2.8, 6.6	3.3	15, 49	0.96

introduction of an OH-group in the mutant L181FY accelerates the transfer twofold.

The temperature dependence of the *P**-decay was measured for wild-type RCs, the mutants M195YF, L181FY, L168HF, M208YF, and for the double mutant L181FY/M208YF (for a summary of the data see Fig. 4 and Table 3). Whereas WT and the mutants M195YF, L181FY, and L168HF show an accelerated *P**-decay at lower temperatures, the double mutant has a temperature-independent decay with a time constant $\tau_{1a} = 3$ ps. For the mutant M208YF the dominant component τ_{1b} slows down from 50 ps at room temperature to 90 ps at 100 K.

At probing wavelengths around 940 to 970 nm, i.e., at the center of the $Q_Y(P)$-band, the decay of *P** and the recovery of the ground state absorption of *P* is measured. In WT RC (dotted lines in Fig. 3) the bleaching of the $Q_Y(P)$ absorption remains constant apart from a small contribution of stimulated emission in the picosecond range, i.e., nearly all *P** are converted to the P^+ product. In mutants with a slow *P** decay ($\tau_1 > 12$ ps; e.g., M208YL, M208YF) a considerable part of the ground state absorption recovers on the picosecond-time scale (Fig. 3, *B* and *C*) pointing to a decreased formation of P^+. Mutants with a shorter lifetime of *P** ($\tau_1 < 10$ ps) show the same behavior as WT RC (for example L181FY, Fig. 3 *A*). The levels reached after a delay time of 1 ns indicate that the quantum yield for $P^+Q_A^-$ formation of ~97% in WT RC (Trissl et al., 1990) is reduced to 65 ± 10% (M208YL) and 75 ± 10% (M208YF) in the mutants. Because the direct recombination times from the intermediate states $P^+H_A^-$ and $P^+Q_A^-$ in wild-type RC are in the nanosecond- and millisecond-time range, respectively (Ogrodnik et al., 1988), the reduced quantum yield after 1 ns must be due to recombination events via early intermediate states (see below).

DISCUSSION

In this paper we have studied the primary step of the ET reaction in WT RCs from *B. viridis* and in 12 mutants. The data are supplemented by the low temperature data on WT and five mutant RCs. The different mutations lead to a considerable change in the primary reaction dynamics. A speeding up of the ET to a reaction time at low temperatures of 250 fs was observed as well as a slowing down to time constants of 90 ps.

ET in photosynthetic RC is usually treated by the nonadiabatic theory, where three important parameters, the electronic coupling *V*, the reorganization energy λ, and the

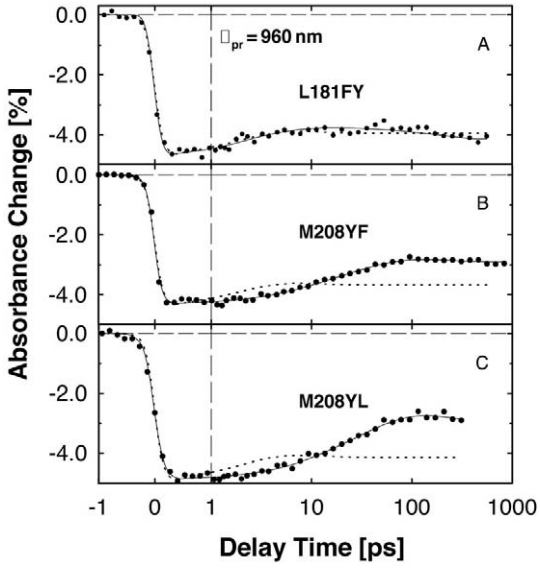

FIGURE 3 Transient absorption data at 960 nm close to the peak of the *P* absorption band for three mutants and the WT RC of *B. viridis* (*points*). The solid curves are model functions using the time constants τ_{1A} and τ_{1B} in Table 2.

gain in free energy ΔG determine the reaction rate. Several publications have evaluated the effect of mutations on the reaction dynamics. In most cases the mutation was assumed to predominantly influence the gain in free energy ΔG (Jia et al., 1993; Bixon et al., 1995).

After a general description of ET theory we will describe the ET reaction in the reaction centers using the approach with constant λ and V. However, we will show that the temperature-dependent ET rates cannot be explained within this model, and we suggest that the mutations strongly influence the electronic coupling.

Theoretical description of ET reactions

To obtain information on the molecular parameters of the first reaction step we will discuss the dominant component τ_{1A} of the biexponential decay function with the help of nonadiabatic electron transfer theory (Marcus and Sutin, 1985; Bixon et al., 1991). In the high temperature limit, the transfer rate constant k depends on the free energy difference ΔG between the product and reactant states, and the temperature T according to the expression

$$k = \frac{2\pi}{\hbar} FC \times V^2 = \frac{2\pi}{\hbar} \frac{1}{\sqrt{4\pi\lambda k_B T}} \exp\left(-\frac{(\Delta G + \lambda)^2}{4\lambda k_B T}\right) \times V^2 \qquad (2)$$

in which FC is the Franck-Condon factor, λ the reorganization energy, and V the electronic coupling matrix element (Marcus and Sutin, 1985). According to Eq. 2 the logarithm of the rate plotted as a function of the free energy difference ΔG is a parabola (Marcus parabola): the rate k reaches a maximum for $\Delta G = -\lambda$ (nonactivation case). The region with $-\Delta G < \lambda$ is called the activated or normal region, whereas the region $-\Delta G > \lambda$ is known as inverted region. The classical Marcus expression for the high temperature Franck-Condon factor is modified if the available excess energy is transferred into additional intramolecular vibrational modes with nonvanishing Franck-Condon factors. This model is required for the description of energetic situations where the first intermediate is well below the electron donor. These modes are considered via an effective high frequency mode ω_H. In this model the Franck-Condon factor in the high temperature limit $k_B T \gg \hbar\omega$ is given by (Bixon et al., 1988):

$$FC = \frac{1}{\sqrt{4\pi\lambda k_B T}} \exp(-S_H) \sum_{n=0}^{\infty} \frac{S_H^n}{n!} \times \exp\left(-\frac{(\Delta G + \lambda + n\hbar\omega_H)^2}{4\lambda k_B T}\right) \qquad (3)$$

in which ω_H is the frequency and S_H a measure for the coupling of the coupling strength of the high frequency mode. In the following we will use the values $\omega_H = 1500$ cm^{-1} and $S_H = 0.5$ (Bixon et al, 1995).

Temperature dependent ET reactions were only recorded for mutants with small gain in free energy. Therefore we do not consider high frequency modes (single mode picture) and fit the temperature dependent data with the semiclassical Hopfield formula 4, which is simpler to evaluate but yields (for the range of parameters used here) a very good approximation of the exact equation (Hopfield, 1976; DeVault, 1984):

$$FC = \frac{1}{\sqrt{2\pi\sigma^2}} \exp\left(-\frac{(\Delta G + \lambda)^2}{2\sigma^2}\right)$$

with

$$\sigma^2 = \lambda\hbar\omega \coth\left(\frac{\hbar\omega}{2k_B T}\right) \qquad (4)$$

In the nonactivation case this equation is reduced to:

$$FC = \frac{1}{\sqrt{2\pi\sigma^2}} \qquad (5)$$

The single mode picture seems to be justified here, since temperature dependent data were not recorded for mutants with very low lying acceptor states, where high frequency modes have to be considered.

Modeling of the ET reactions, model A: room temperature rates of different mutants fitted with constant *V* and λ

The decay times of the dominant components τ_{1A} of the various mutants are used here to determine the relevant parameters of the primary electron transfer via Eqs. 2 and 3. Because these equations contain a series of reaction parameters, several assumptions are necessary to reduce the number of free parameters. At first we follow the most common approach used for the RCs of *Rb. sphaeroides* and *Rb. capsulatus* (Williams et al., 1992; Jia et al., 1993; Bixon et al., 1995; Zinth et al., 1998). It is supposed that the electronic coupling V and the reorganization energy λ are the same for all mutants. Thus, the mutations act only on the free energy difference ΔG, which can be deduced from the measured P/P^+ midpoint potential. The variations of the $Q_Y(P)$ absorption band are not considered when estimating the energy levels. This procedure is justified, since no large changes occur for mutants of group 2 to 4 and since it has been shown that the observed shifts of the group 1 mutants are not directly correlated with the energy level of P^* (Mattioli et al., 1995; Wachtveitl et al., 1993a). In this model the only relevant parameter to be determined is the energy difference between P^* and $P^+B_A^-$ in the wild-type RC. The absolute energetic positions of all other mutants follow from this value. The absolute energy difference ΔG

between $G_{mut}(P^*)$ and the first transfer product $G_{mut}(P^+I^-)$ of a mutant is given by:

$$\Delta G_{mut}(P^+I^-) = G_{mut}(P^+I^-) - G_{mut}(P^*) = C - \Delta\Delta G(P^+I^-) \quad (6)$$

The abbreviation I refers to the first acceptor in the ET. For a stepwise ET reaction the BChl-b B_A. Here $C = \Delta G_{WT}(P^+I^-)$ is the absolute energy difference between $G(P^+I^-)$ and $G(P^*)$ in WT and $\Delta\Delta G$ the relative energy difference induced by the mutation. The relative changes $\Delta\Delta G$ in the free energy of the first ET step can be estimated for several situations: if the energy level of P* and the molecular nature of the chromophores are not affected by the mutation, the standard free energy change $\Delta\Delta G$ of a P^+ containing intermediate state (P^+I^-) can be estimated by the change of the P/P^+ midpoint redox potential $\Delta U_{P/P^+}$:

$$\Delta\Delta G(P^+I^-) = \Delta G(P^+I^-)_{WT} - \Delta G(P^+I^-)_{mut} \approx -\Delta U_{P/P^+} \quad (7)$$

Here a decrease in redox potential with respect to the WT RC ($\Delta U_{P/P^+} > 0$) corresponds to an increased energy of the intermediate state P^+I^- in the corresponding mutant. It should be noted that influences on the energy of the chromophore I can not be recorded by measuring the P/P^+ redox potential. However, if a mutation leads to the incorporation of a different chromophore, the free energy change can be estimated by:

$$\Delta\Delta G(P^+I^-) \approx -\Delta U_{P/P^+} - \Delta U_{Chrom} \quad (8)$$

in which ΔU_{Chrom} is the in situ difference of the midpoint redox potential of the exchanged chromophores. For those cases, where an estimate of the in vivo difference of the midpoint potential is not possible, it is necessary to use the in vitro value (e.g., in dimethylformamide). Only in the L153HL RC the mutation results in a chromophore exchange and a value of $\Delta U_{Chrom} \neq 0$ has to be considered. Because BPhe-*b* in dimethylformamide has a substantially more negative one-electron reduction potential (−0.5 V) than BChl-*b* (−0.7 V) (Geskes et al., 1995), the insertion of BPhe-*b* into the B_A binding site drastically changes the energetics of the radical pair state $P^+B_A^-$. According to Eq. 6 this corresponds to an energy difference $\Delta\Delta G(P^+B_A^-) \approx -1600\ cm^{-1}$. In this context, it must be noted that the absolute value of a redox midpoint potential strongly depends on the solvent used. However, the difference of the midpoint potentials of two chromophores, which is used here for the energy estimate, does not significantly depend on the solvent.

A reasonable estimate of the real free energy change $\Delta\Delta G$ by the P/P^+ midpoint potential is not possible for every mutant (Bixon et al., 1995). As a consequence we have to discard "poor" mutants. There are two types of mutated RC that are not considered for the energy estimates.

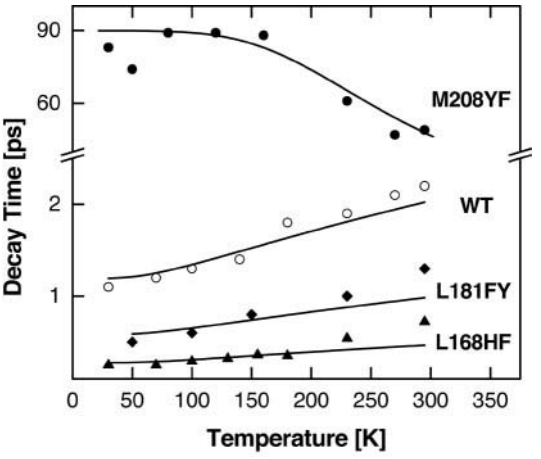

FIGURE 4 Temperature dependence of WT and the mutants M208YF, L181FY, L168HF. Solid curves are calculated with the parameters given in Table 4.

1) Double mutations are supposed to induce larger geometrical changes. For these mutants, it is not possible to maintain the hypothesis of a nearly unchanged electronic coupling V. We will see below that, even for the other mutants, changes in V may become important. 2) Mutants where the modification is not restricted to P/P^+. Here the measured P/P^+ potential is not sensitive to the changes on the other chromophores. The energy estimates within these mutant RCs cannot be accurate. This is the case for the M208 mutants (see below), where we determine ΔG from the temperature dependence (Fig. 4). For L153HL RC, the energetic changes on B_A can be accounted for by the redox potential of the introduced bacteriopheophytin (Eq. 6).

The estimated relative energy changes $\Delta\Delta G$ (according to Eqs. 7 and 8 of the selected mutants are shown in Table 1. These values, the observed decay constants τ_{1A} and Eqs. 2 and 6 yield a data set with 9 equations and the 3 unknown parameters λ, V_1 and C. A least squares fit produces a Marcus parabola (Eq. 2) with the following parameters: $\lambda = 600\ cm^{-1} \pm 200\ cm^{-1}$, $V = 30\ cm^{-1} \pm 8\ cm^{-1}$, and $C = -55 \pm 250\ cm^{-1}$.

Because $G(P^+H_A^-)$ is known to lie between 1600 cm^{-1} and 2000 cm^{-1} below $G(P^*)$ (Ogrodnik et al., 1994), one important consequence of a value $C = \Delta G(P^+I^-)_{WT} = -55\ cm^{-1}$ is that the first electron transfer product cannot be $P^+H_A^-$ and must therefore be $P^+B_A^-$.

The measured decay constants τ_{1A} versus the estimated energy differences are plotted together with the modeled Marcus parabola in Fig. 5 (broken curve). The minimum of the parabola is at $\Delta G = -\lambda = -600\ cm^{-1}$. Interestingly, this procedure places the WT RC in the activated region of the curve. On the other side, the introduction of a bacteriopheophytin instead of the bacteriochlorophyll at the site B_A in the L153HL mutant places the primary electron transfer reaction of this RC in the inverted region. The good agree-

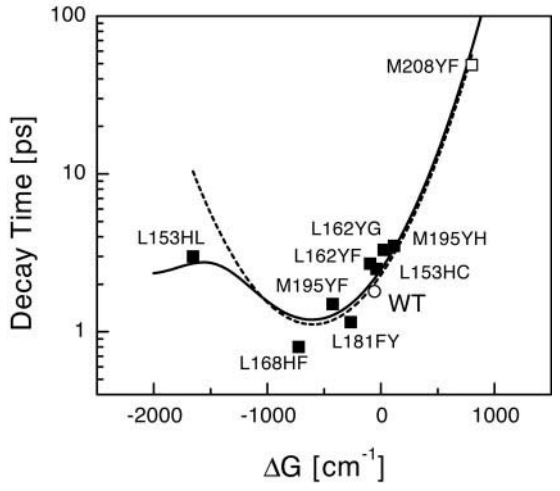

FIGURE 5 Visualization of the reaction parameters deduced from the different mutants at room temperature using the assumptions of the model A. (*Points*) P^* decay time of the dominant component plotted versus $\Delta G(P^+B_A^-)$ energies estimated by the midpoint potentials. The absolute energy scale was deduced from the fitting procedure. For M208YF, ΔG was determined from the change of τ_{1B} with temperature (Table 4). (*Solid line*) Marcus parabola for one high frequency mode. (*Broken curve*) Single mode model. It should be noted that model A fails to explain the temperature dependence of the reaction rates (see text).

ment between most room temperature data points and the modeled parabola could be used as a justification for the assumption of nearly constant values of λ and V for the selected "good" mutants.

If the multimode model is used to fit the data, we obtain the solid curve in Fig. 5 *a*. A least squares fit using Eq. 3 and $\omega_H = 1500\ cm^{-1}$ and $S_H = 0.5$ yields values of $\lambda = 600\ cm^{-1} \pm 200\ cm^{-1}$, $V = 37\ cm^{-1} \pm 10\ cm^{-1}$, and $C = -55 \pm 250\ cm^{-1}$. The most striking difference between the classical parabola and the multimode case is that in the latter case the mutant L153HL is much closer to the theoretical curve. In conclusion, both models yield reasonable results and can explain the room temperature data.

The ET parameters for most RCs, especially for the wild-type RC, correspond to a thermal activation of the primary ET reaction step (Eq. 2). From the reorganization energy and the free energy difference obtained in the classical Marcus case and in the multimode picture, we can estimate an activation energy $E_A = (\Delta G(P^+B_A^-)_{WT} + \lambda)^2/4\lambda \approx 180\ cm^{-1}$ for the WT RC. In the single mode picture, this activation energy would slow down the primary ET steps significantly when the sample is cooled. For most other mutants the primary reaction is also activated, and a similar slowing down is expected. It should be noted that in the case of a significant gain in free energy ($|\Delta G| \gg \lambda$, inverted region) the multimode model could avoid the slowing down of the primary ET reaction at lower temperatures for a specific choice of the reaction parameters. However, the small gain in free energy in the investigated mutants do not favor this explanation for ET to B_A. Structural reorganization of a network of water molecules associated with the slower rereduction of P^+ by cytochrome were suggested to explain the temperature dependence of this slow ($\approx 10^{-6}$ μs) ET reaction (Ortega et al., 1998).

Even if we cannot fully rule out changes in reorganization energy λ as an influence upon the primary reaction, the rigid environment of the primary electron carriers (Deisenhofer and Michel, 1989) requires an alternative explanation. Therefore, a temperature dependence of the reorganization energy λ will not be discussed in the following.

Modeling of the ET reactions, model B: temperature dependence of the initial electron transfer reaction fitted with temperature independent parameters

The primary reactions (dominating component) of various RCs (WT, L181FY, M195YF, L168HF) are accelerated at low temperatures. Therefore, these reaction centers should have negligible activation energies $E_A \ll \hbar\omega$. Since this observation is in contradiction with the activation energies calculated above in section B, we have to consider alternative reaction parameters compatible with the experimentally observed temperature dependencies. To simplify the analysis, we first assume that the reorganization energy (the same value $\lambda = 600\ cm^{-1} \pm 200\ cm^{-1}$ is used for all mutants) and the various electronic couplings are independent of temperature. The analysis yields a qualitative description of the temperature dependencies with $\lambda = 600$, $\hbar\omega = 150\ cm^{-1}$ for all samples. Here $\hbar\omega$ was determined from the temperature dependence of the nonactivated mutants at low temperatures (<100 K), where no deviation from the theoretical model is found. The individual free energies and electronic couplings of the different mutants are given in columns 3 and 4 of Table 4. As expected, the results for ΔG are inconsistent with the analysis according to model A (see Table 4, column 2). In addition, the electronic couplings vary considerably upon mutation. Even with these temperature-independent parameters the experimental data and model curves do not agree perfectly (see Fig. 4, at higher temperatures). Often the observed acceleration of the reaction rates toward low temperatures is higher than described even by the activationless ET theory. This discrepancy may result from the assumption of temperature-independent electronic couplings. Indeed, the experimental data of Fig. 4 may be well modeled if the couplings V decrease gradually between 150 and 300 K.

M208YF is the only mutant studied that shows a slowing down of the ET reaction at lower temperatures. The simulation of this temperature dependence simply by using Eq. 4, however, is not successful, as a strong increase in reaction time at temperatures between 300 and 150 K requires a high activation energy, which would lead to an even stronger increase in reaction time at the lower temperatures. The

TABLE 4 Electron transfer parameters for the primary ET step deduced via different models

	ΔG (cm^{-1}) (from model A, room temperature data, and constant V and λ	ΔG (cm^{-1}) (from the temperature dependence of the primary ET-step with constant λ and $\hbar\omega$)	V (cm^{-1})
WT	−55	−600	23
L168HF	−725	−600	48
L181FY	−265	−600	33
M195YF	−425	−600	25
L181FYM208YF	-	−300	9
L153HC	−39	-	-
L162YF	−95	-	-
L153HL	−1655	-	-
L162YG	25	-	-
M195YH	115	-	-
M208YF	(800)	800	22

Column 2, Values for ΔG obtained using model A (Eq. 2) with $\lambda = 600$ $cm^{-1} \pm 200$ cm^{-1} and $V = 30$ $cm^{-1} \pm 8$ cm^{-1}. Column 3 and 4, The temperature dependence of the dominant component in primary ET is used to deduce temperature independent values for ΔG and V (Eq. 4) with $\lambda = 600$ $cm^{-1} \pm 200$ cm^{-1} and $\hbar\omega = 150$ cm^{-1}.

leveling of the reaction time suggests that at low temperatures another reaction channel with $\tau \cong 90$ ps dominates the decay of P^*. The fitting curve in Fig. 4 uses two decay channels for P^*: the first one is thermally activated ET according to Eq. 4 with the parameters given in Table 4, whereas the second one is temperature independent with $\tau = 90$ ps. This additional decay path of P^* may be connected with an internal conversion of P^* to ground state P or to a direct superexchange ET to state $P^+H_A^-$ (Bixon et al., 1995).

Towards more consistent reaction models

In the discussion above several assumptions have been made to reduce the number of free parameters for the modeling of the ET reaction for different mutants and different temperatures. From the contradictory values of the reaction parameters, which result with simplifying model assumptions we can conclude that these assumptions are not adequate to describe photosynthetic ET. As a consequence, only qualitative conclusions may be drawn about the reaction parameters. For example, the low temperature data indicate that the electronic coupling for the first ET reaction is influenced by the temperature change. Considering this observation, it becomes evident that mutations with weak structural changes may also modify the electronic coupling V. Thus, the commonly used strategy underlying model A is inadequate, and the results on the energetics deduced from model A (see Fig. 5 for RC of *B. viridis*) have to be questioned. For the RCs of *Rb. sphaeroides* and *Rb. capsulatus* (Williams et al., 1992; Jia et al., 1993; Bixon et al., 1995; Zinth et al., 1998) similar arguments may apply.

Nevertheless, the analysis of the different mutated RCs at different temperatures yields an important qualitative insight to the reaction parameters, as only certain combinations of parameters are consistent with the observations.

Electronic coupling V

The experiments indicate that V varies with mutation and temperature. Apparently both processes influence the structural (nuclear and electronic) arrangement of the RC. The high sensitivity of V to subtle conformational rearrangements leads to significant changes of the ET dynamics (Kolbasov and Scherz, 2000). From the present experiments, we conclude that the value of V for wild-type RC of *B. viridis* should be of the order of 20 to 35 cm^{-1}.

Reorganization energy λ

Small values of λ make the electron transfer reaction very sensitive to changes in free energy ΔG. On the other hand, large values of λ require a large gain in free energy to ascertain an activationless reaction which requires $\Delta G = -\lambda$. The numerous model calculations and the known energetics of intermediate $P^+H_A^-$ place λ for the initial ET of the wild-type RC in the range of $\lambda = 800 - 400$ cm^{-1}. Stronger deviations from this value lead to inconsistencies when describing temperature or mutation dependencies. To some extent, λ may vary with temperature or mutation, however a systematic dependence could not be found.

Gain in free energy ΔG

In many publications it was assumed that the most sensitive parameter of the ET is ΔG. As shown above, several mutant RCs react activationless even if the procedure to determine ΔG from model A yielded significant differences. For a consistent picture one has to suppose that the model assumptions used in model A (V and λ set to be constant) are inadequate and, as a consequence, the calculated reaction parameters, especially the energetics, (see Fig. 5) do not always reflect reality. At the present state of the experiments it appears that only qualitative conclusions can be drawn on the energetics, placing some mutants (M208YF, M208YL) well above the wild-type RCs, others below or close to wild type, which should be nearly activationless, $\Delta G \sim -\lambda$.

Optimization of the primary reaction

For high quantum efficiencies η of the total photosynthetic reaction chain (it has been shown for WT *B. viridis* that η amounts to 97% (Trissl et al., 1990)) the primary reaction steps themselves have to occur with highest quantum efficiency η_{P^*} for initial charge separation. Quantum efficiency in the very first step is reduced if competing recombination channels (with rates γ_{10}) reduce the probability of success-

ful charge separation processes. For a first step with an ET rate γ_{12} η_{P*} can be estimated to be: $\eta_{P*} = \gamma_{12}/(\gamma_{12} + \gamma_{10})$. When the ET rate γ_{12} is reduced (at a fixed recombination rate γ_{10}), the quantum efficiency drops and the decay of *P** (rate $\gamma_1 = 1/\tau_1 = \gamma_{12} + \gamma_{10}$) is slowed down (Gray et al. 1990). The presented absorbance changes in the $Q_Y(P)$ band of the M208 mutants at room temperature (Fig. 3) indicate that such a direct ground state recombination is important in the RC of *B. viridis*. The slow primary charge separation reaction in the M208YF and M208YL mutants is connected with an increase of the ground state recombination yield. The change in the long lasting absorbance observed in the special pair band (see Fig. 3) has been used to determine the quantum yield in the M208YL and M208YF mutants to be $\sim$ 65% $\pm$ 10% and 75% $\pm$ 10%, respectively. These data point to a direct ground state recombination rate of $\gamma_{10} \approx 1/(80\text{ ps} \pm 30\text{ ps})$. The additional decay channel used to explain the reaction time at low temperatures in the mutant M208YF of $\tau_1 = 90$ ps would be in full agreement with this finding. However, the treatment (by glycerol and benzyl viologen) of the samples used for the low temperature experiments may influence the absorption dynamics at long delay times. Therefore, we cannot finally decide if the limiting $\tau = 90$ps process necessary to fit the data of M208YF at low temperatures is related with internal conversion or with a direct superexchange ET to the BPhe-*a* H_A.

Considering the efficiency η_{P*} of the first ET step, it is surprising that evolution did not lead to a RC corresponding to the mutant L168HF, where η_{P*} is somewhat larger than in WT RC. In this context it should be taken into consideration that the efficiency of photosynthesis in a bacterium does not only depend upon the efficiency of the initial reaction. For a linear reaction model of the photo-induced reactions in photosynthesis, the overall efficiency of the total reaction chain depends on the forward and backward reaction of each step including the energy transfer from the light harvesting complex. To obtain an efficient energy transfer from the antenna to *P** the energetic levels of the two pigment-protein complexes have to be adjusted for optimum excitation transfer. Apparently, this energy transfer is optimized for the absorption spectrum of WT RC, whereas for the fast-reacting mutant L168HF where the *P*-band (see absorption peak given in Table 1) lies at shorter wavelengths than in WT, the energy transfer efficiency from the low lying antenna to the RC should be reduced (Arlt et al., 1996a). As a consequence, the effect of the increased reaction speed, which would slightly improve the quantum efficiency for primary charge separation in the reaction center itself, (from 97% to 98.8%) is largely overcompensated by the loss due to poorer excitation transfer from the antenna.

CONCLUSION

The large number of mutated RCs discussed in this paper has allowed us to investigate primary photosynthesis in *B. viridis* over a wide range of time constants from 250 fs to 90 ps. If hydrogen bonds to the special pair are removed, a drastic acceleration of the first transfer step is observed. On the other hand, we found a slowing down of the *P** decay times in mutants, where tyrosine M208 was replaced by nonpolar amino acids, which agrees with the results on *Rb. sphaeroides* (Nagarajan et al., 1990; Finkele et al., 1990). These slowly reacting mutants have a reduced quantum efficiency for charge separation, which point to a recombination channel from *P** in the 80 to 100-ps time domain. An evaluation of the whole data set within the framework of nonadiabatic theory reveals that the commonly made assumption of a constant electronic coupling V for all mutants and over the whole temperature range is not correct (in accordance with recent theoretical arguments Kolbasov and Scherz, 2000). One may therefore conclude that a simple relationship between mutation and a change in one reaction parameter cannot be given and that at least the electronic coupling is changed upon mutation.

Qualitatively, the reaction parameters for the wild-type RC are similar for *B. viridis* and *Rb. sphaeroides* with values of $V = 20$ to 35 cm^{-1}, $\lambda = 400$ to 800 cm^{-1}, and nonactivated electron transfer $\Delta G \approx -\lambda$. The investigations convincingly show that the primary reactions of *B. viridis*, i.e., a purple bacterium which uses BChl-*b* and BPhe-*b* as electron carriers and has accessed the ecological niche using light beyond 1000 nm, behaves very similarly to the other reaction centers such as *Rb. sphaereoides* where BChl-*a* and BPhe-*a* are used instead of BChl-*b* and BPhe-*b*. Not only are the reaction dynamics similar, but mutations also lead to similar changes in the different species. The results show that unique design criteria are used for the reaction centers of the different bacteria.

REFERENCES

Arlt, T., M. Bibikova, H. Penzkofer, D. Oesterhelt, and W. Zinth. 1996a. Strong acceleration of primary photosynthetic electron transfer in a mutated reaction center of *Rhodopseudomonas viridis*. *J. Phys. Chem.* 100:12060–12065.

Arlt, T., B. Dohse, S. Schmidt, J. Wachtveitl, E. Laußermair, W. Zinth, and D. Oesterhelt. 1996b. Electron transfer dynamics of *Rps. viridis* reaction centers with a modified binding site for the accessory bacteriochlorophyll. *Biochemistry.* 35:9235–9244.

Arlt, T., S. Schmidt, W. Kaiser, C. Lauterwasser, M. Meyer, H. Scheer, and W. Zinth. 1993. The accessory bacteriochlorophyll: a real electron carrier in primary photosynthesis. *Proc. Natl. Acad. Sci. U.S.A.* 90: 11757–11761.

Beekman, L. M. P., I. H. M. van Stokkum, R. Monshouwer, A. J. Rijnders, P. McGlynn, R. W. Visschers, M. R. Jones, and R. van Grondelle. 1996. Primary electron-transfer in membrane-bound reaction centers with mutations at the M210 position. *J. Phys. Chem.* 100:7256–7268.

Beekman, L. M. P., R. W. Visschers, R. Monshouwer, M. Heer-Dawson, T. A. Mattioli, P. McGlynn, C. N. Hunter, B. Robert, I. H. M. van Stokkum, R. van Grondelle, and M. R. Jones. 1995. Time-resolved and steady-state spectroscopic analysis of membrane-bound reaction centers from *Rhodobacter sphaeroides:* comparisons with detergent-solubilized complexes. *Biochemistry.* 34:14712–14721.

Bixon, M., J. Jortner, and M. E. Michel-Beyerle. 1988. Radical pair dynamics in the bacterial photosynthetic reaction center. *In* The Photosynthetic Bacterial Reaction Center II: Structure, Spectroscopy and

Dynamics. J. Breton and A. Verméglio, editors. Plenum Press, New York. 283–290.

Bixon, M., J. Jortner, and M. E. Michel-Beyerle. 1991. On the mechanism of the primary charge separation ion bacterial photosynthesis. *Biochim. Biophys. Acta.* 1056:301–315.

Bixon, M., J. Jortner, and M. E. Michel-Beyerle. 1995. A kinetic analysis of the primary charge separation in bacterial photosynthesis: energy gaps and static heterogeneity. *Chem. Phys.* 197:389–404.

Breton, J., J. L. Martin, A. Migus, A. Antonetti, and A. Orszag. 1986. Femtosecond spectroscopy of excitation energy transfer and initial charge separation in the reaction center of the photosynthetic bacterium *Rhodopseudomonas viridis*. *Proc. Natl. Acad. Sci. U.S.A.* 83:5121–5125.

Bylina, E. J., C. Kirmaier, L. McDowell, D. Holten, and D. C. Youvan. 1988. Influence of an amino-acid residue on the optical properties and electron transfer dynamics of a photo-synthetic reaction center complex. *Nature.* 336:182–184.

Deisenhofer, J., and H. Michel. 1989. The photosynthetic reaction centre from the purple bacterium *Rhodopseudomonas viridis*. *EMBO J.* 8:2149–2170.

DeVault, D. 1984. Quantum Mechanical Tunneling in Biological Systems. University Press, Cambridge, MA.

Ditta, G., T. Schmidhauser, E. Yakobson, P. Lu, X. W. Liang, D. R. Finlay, D. Guiney, and D. R. Helsinki. 1985. Plasmids related to the broad host range vector, pRK290, useful for the cloning and monitoring gene expression. *Plasmid.* 13:149–153.

Dohse, B., P. Mathis, J. Wachtveitl, E. Laußermair, S. Iwata, H. Michel, and D. Oesterhelt. 1995. Electron transfer from the tetraheme cytochrome to the special pair in the *Rhodopseudomonas viridis* reaction centre: effect of mutations of tyrosine L162. *Biochemistry.* 34: 11335–11343.

Dressler, K., E. Umlauf, S. Schmidt, P. Hamm, W. Zinth, S. Buchanan, and H. Michel. 1991. Detailed studies of the subpicosecond kinetics in the primary electron transfer of reaction centers of *Rhodopseudomonas viridis*. *Chem. Phys. Lett.* 183:270.

Du, M., S. J. Rosenthal, X. Xie, T. J. Dimagno, M. Schmidt, D. K. Hanson, M. Schiffer, J. R. Norris, and G. R. Fleming. 1992. Femtosecond spontaneous-emission studies of reaction centers from photosynthetic bacteria. *Proc. Natl. Acad. Sci. U.S.A.* 89:8517–8521.

Ermler, U., G. Fritzsch, S. K. Buchanan, and H. Michel. 1994. Structure of the photosynthetic reaction centre from *Rhodobacter sphaeroides* at 2.65 A resolution: cofactors and protein-cofactor interactions. *Structure.* 2:925–936.

Farchaus, J. W., J. Wachtveitl, P. Mathis, and D. Oesterhelt. 1993. Tyrosine-162 of the photo-synthetic reaction-center L-subunit plays a critical role in the cytochrome-C2 mediated rereduction of the photooxidized bacteriochlorophyll dimer in rhodobacter-sphaeroides: I. Site-directed mutagenesis and initial characterization. *Biochemistry.* 32: 10885–10893.

Finkele, U., C. Lauterwasser, W. Zinth, K. A. Gray, and D. Oesterhelt. 1990. The role of tyrosine M210 in the initial charge separation of reaction centers of *Rhodobacter sphaeroides*. *Biochemistry.* 29: 8517–8521.

Fleming, G. R., J. L. Martin, and J. Breton. 1988. Rates of primary electron-transfer in photosynthetic reaction centers and their mechanistic implications. *Nature.* 333:190–192.

Geskes, C., G. Hartwich, H. Scheer, W. Maentele, and J. Heinze. 1995. Electrochemical and spectroelectrochemical investigation of metal-substituted bacteriochlorophyll a. *J. Am. Chem. Soc.* 117:7776–7783.

Gray, K. A., J. W. Farchaus, J. Wachtveitl, J. Breton, and D. Oesterhelt. 1990. Initial characterization of site-directed mutants of tyrosine M210 in the reaction centre of *Rhodobacter sphaeroides*. *EMBO J.* 9:2061–2070.

Hamm, P., K. A. Gray, D. Oesterhelt, R. Feick, H. Scheer, and W. Zinth. 1993. Subpicosecond emission studies of bacterial reaction centers. *Biochim. Biophys. Acta.* 1142:99–105.

Heller, B. A., D. Holten, and C. Kirmaier. 1995. Control of electron transfer between the L-and M-sides of photosynthetic reaction centers. *Science.* 269:940–945.

Holzapfel, W., U. Finkele, W. Kaiser, D. Oesterhelt, H. Scheer, H. U. Stilz, and W. Zinth. 1989. Observation of a bacteriochlorophyll anion radical during the primary charge separation in a reaction center. *Chem. Phys. Lett.* 160:1.

Holzapfel, W., U. Finkele, W. Kaiser, D. Oesterhelt, H. Scheer, H. U. Stilz, and W. Zinth. 1990. Initial electron transfer in the reaction center from *Rhodobacter sphaeroides*. *Proc. Natl. Acad. Sci. U.S.A.* 87:5168–5172.

Hopfield, J. 1976. Fundamental aspects of electron transfer in biological membranes. *In* Phénoménes électrique au niveau des membrane biologique. *29th Int. Congr. Societé Chimie Phys.* E. Roux, editor. Elsevier, Amsterdam. 471–492.

Huber, H., M. Meyer, H. Scheer, W. Zinth, and J. Wachtveitl. 1998. Temperature dependence of the primary electron transfer reaction in pigment-modified bacterial reaction centers. *Photosynth. Res.* 55: 153–162.

Jia, Y. W., T. J. DiMagno, C. K. Chan, Z. Y. Wang, M. Du, D. K. Hanson, M. Schiffer, J. R. Norris, G. R. Fleming, and M. S. Popov. 1993. Primary charge separation in mutant reaction centers of rhodobacter capsulatus. *J. Phys. Chem.* 97:13180–13191.

Kolbasov, D., and A. Scherz. 2000. Asymmetric electron transfer in reaction centers of purple bacteria strongly depends on different electron matrix elements in the active and inactive branches. *J. Phys. Chem. B.* 104:1802–1809.

Kuglstatter, A., P. Hellwig, G. Fritzsch, J. Wachtveitl, D. Oesterhelt, W. Mäntele, and H. Michel. 1999. Identification of a hydrogen bond in the Phe M197 → Tyr mutant reaction center of the photosynthetic purple bacterium *Rhodobacter sphaeroides* by X-ray crystallography and FTIR spectroscopy. *FEBS Lett.* 463:169–174.

Lancaster C.R. M.V. Bibikova, P. Sabatino, D. Oesterhelt, and H. Michel. 2000. Structural basis of the drastically increased initial electron transfer rate in the reaction center from a *Rhodopseudomonas viridis* mutant described at 2.00-A resolution. *J. Biol. Chem.* 275:39364–39368.

Lancaster, C. R., and H. Michel. 1997. The coupling of light-induced electron transfer and proton uptake as derived from crystal structures of reaction centres from *Rhodopseudomonas viridis* modified at the binding site of the secondary quinone, Q_B. *Structure.* 5:1339–1359.

Laußermair, E., and D. Oesterhelt. 1992. A system for site-specific mutagenesis of the photo-synthetic reaction center in *Rhodopseudomonas viridis. EMBO J.* 11:777–783.

Lauterwasser, C., U. Finkele, H. Scheer, and W. Zinth. 1991. Temperature dependence of the primary electron transfer in photosynthetic reaction centers from *Rhodobacter sphaeroides. Chem. Phys. Lett.* 183:471–477.

Marcus, R. A., and N. Sutin. 1985. Electron transfers in chemistry and biology. *Biochim. Biophys. Acta.* 811:265–322.

Mattioli, T. A., X. Lin, J. P. Allen, and J. C. Williams. 1995. Correlation between multiple hydrogen bonding and alteration of the oxidation potential of the bacteriochlorophyll dimer of reaction centers from *Rhodobacter sphaeroides. Biochemistry.* 34:6142–6152.

Murchison, H. A., R. G. Alden, J. P. Allen, J. M. Peloquin, A. K. Taguchi, N. W. Woodbury, and J. C. Williams. 1993. Mutations designed to modify the environment of the primary electron donor of the reaction center from *Rhodobacter sphaeroides*: phenylalanine to leucine at L167 and histidine to phenylalanine at L168. *Biochemistry.* 32:3498–3505.

Nagarajan, V., W. W. Parson, D. Davis, and C. C. Schenck. 1993. Kinetics and free energy gaps of electron-transfer reactions in *Rhodobacter sphaeroides* reaction centers. *Biochemistry.* 32:12324–12336.

Nagarajan, V., W. W. Parson, D. Gaul, and C. Schenck. 1990. Effect of specific mutations of tyrosine-(M)210 on the primary photosynthetic electron-transfer process in *Rhodobacter sphaeroides*. *Proc. Natl. Acad. Sci. U.S.A.* 87:7888–7892.

Ogrodnik, A., W. Keupp, M. Volk, G. Aumeier, and M. E. Michel-Beyerle. 1994. Inhomogeneity of radical pair energies in photosynthetic reaction centers revealed by differences in recombination dynamics of $P^+H_A^-$ when detected in delayed emission and in absorption. *J. Phys. Chem.* 98:3432–3439.

Ogrodnik, A., M. Volk, and M. E. Michel-Beyerle. 1988. On the energetics of states $^1P^*$, $^3P^*$ and P^+H^- in reaction centers of *Rb. sphaeroides*. *In* The Photosynthetic Bacterial Reaction Center - Structure and Dynamics. J. Breton and A. Verméglio, editors. Plenum Press, New York. 177–184.

Ortega, J. M., B. Dohse, D. Oesterhelt, and P. Mathis. 1998. Low-temperature electron transfer from cytochrome to the special pair in *Rhodopseudomonas viridis*: role of the L162 residue. *Biophys. J.* 74: 1135–1148.

Parson, W. W., Z. T. Chu, and A. Warshel. 1990. Electrostatic control of charge separation in bacterial photosynthesis. *Biochim. Biophys. Acta.* 1017:251–272.

Parson, W. W., and A. Warshel. 1993. Simulations of electron transfer in bacterial reaction centers. *In* The Photosynthetic Reaction Center. J. Deisenhofer and J. R. Norris, editors. Academic Press, San Diego, CA. 239–249.

Schmidt, S., T. Arlt, P. Hamm, H. Huber, T. Nagele, J. Wachtveitl, M. Meyer, H. Scheer, and W. Zinth. 1994. Energetics of the primary electron-transfer reaction revealed by ultrafast spectroscopy on modified bacterial reaction centers. *Chem. Phys. Lett.* 223:116–120.

Schmidt, S., T. Arlt, P. Hamm, H. Huber, T. Nägele, J. Wachtveitl, W. Zinth, M. Meyer, and H. Scheer. 1995. Primary electron-transfer dynamics in modified bacterial reaction centers containing pheophytin-a instead of bacteriopheophytin-a. *Spectrochim. Acta.* 51:1565–1578.

Schmidt, S., T. Arlt, P. Hamm, C. Lauterwasser, U. Finkele, G. Drews, and W. Zinth. 1993. Time-resolved spectroscopy of the primary photosynthetic processes of membrane-bound reaction centers from an antenna-deficient mutant of *Rhodobacter* capsulatus. *Biochim. Biophys. Acta.* 1144:385–390.

Spörlein, S., W. Zinth, M. Meyer, H. Scheer, and J. Wachtveitl. 2000. Primary electron transfer in modified bacterial reaction centers: optimization of the first events in photosynthesis. *Chem. Phys. Lett.* 322: 454–464.

Spörlein, S., W. Zinth, and J. Wachtveitl. 1998. Vibrational coherence within the bacteriochlorophyll anion band of *Rb. sphaeroides* reaction centers. *J. Phys. Chem.* 102:7492–7496.

Trissl, H. W., J. Breton, J. Deprez, A. Dobek, and W. Leibl. 1990. Trapping kinetics annihilation and quantum yield in the photosynthetic bacterium *Rhodopseudomonas viridis* as revealed by electric measurement of the primary charge separation. *Biochim. Biophys. Acta.* 1015:322–333.

Vos, M. H., J. C. Lambry, S. J. Robles, D. C. Youvan, J. Breton, and J. L. Martin. 1991. Direct observation of vibrational coherence in bacterial reaction centers using femtosecond absorption spectroscopy. *Proc. Natl. Acad. Sci. U.S.A.* 88:8885–8889.

Vos, M. H., J. C. Lambry, S. J. Robles, D. C. Youvan, J. Breton, and J. L. Martin. 1992. Femtosecond spectral evolution of the excited state of bacterial reaction centers at 10 K. *Proc. Natl. Acad. Sci. U.S.A.* 89: 613–617.

Vos, M. H., F. Rappaport, J. C. Lambry, J. Breton, and J. L. Martin. 1993. Visualization of coherent nuclear motion in a membrane-protein by femtosecond spectroscopy. *Nature.* 363:320–325.

Wachtveitl, J., J. W. Farchaus, R. Das, M. Lutz, B. Robert, and T. A. Mattioli. 1993a. Structure, spectroscopic, and redox properties of *Rhodobacter sphaeroides* reaction centers bearing point mutations near the primary electron donor. *Biochemistry.* 32:12875–12886.

Wachtveitl, J., J. W. Farchaus, P. Mathis, and D. Oesterhelt. 1993b. Tyrosine-162 of the photosynthetic reaction-center L-subunit plays a critical role in the cytochrome-c_2 mediated rereduction of the photooxidized bacteriochlorophyll dimer in *Rhodobacter sphaeroides:* II. Quantitative kinetic analysis. *Biochemistry.* 32:10894–10904.

Wachtveitl, J., H. Huber, R. Feick, J. Rautter, F. Muh, and W. Lubitz. 1998. Electron transfer in bacterial reaction centers with an energetically raised primary acceptor: ultrafast spectroscopy and ENDOR/TRIPLE studies. *Spectrochim. Acta.* 54:153–162.

Williams J.C., R.G. Alden, H.A. Murchison, J.M. Peloquin, N.W. Woodbury, and J.P. Allen. 1992. Effects of mutations near the bacteriochlorophylls in reaction centers from *Rhodobacter sphaeroides*. *Biochemistry.* 31:11029–11037.

Woodbury, N. W., S. Lin, X. M. Lin, J. M. Peloquin, A. K. W. Taguchi, J. C. Williams, and J. P. Allen. 1995. The role of reaction-center excited-state evolution during charge separation in a *Rhodobacter sphaeroides* mutant with an initial electron-donor midpoint potential 260 Mv above wild-type. *Chem. Phys.* 197:405–421.

Woodbury, N. W., J. M. Peloquin, R. G. Alden, X. Lin, S. Lin, A. K. Taguchi, J. C. Williams, and J. P. Allen. 1994. Relationship between thermodynamics and mechanism during photoinduced charge separation in reaction centers from *Rhodobacter sphaeroides*. *Biochemistry.* 33: 8101–8112.

Zinth W., P. Huppmann, T. Arlt, and J. Wachtveitl. 1998. Ultrafast spectroscopy of the electron transfer in photosynthetic reaction centers: towards a better understanding of electron transfer in biological systems. *Phil. Trans. R. Soc. Lond. A.* 356: 465–476.